

Synthesis and photochemical properties of azidohemicyanine

M. F. Budyka,^{a*} N. V. Biktimirova,^a T. N. Gavrishova,^a and V. I. Kozlovskii^b

^a*Institute of Problems of Chemical Physics, Russian Academy of Sciences,
1 prosp. Akad. Semenova, 142432 Chernogolovka, Moscow Region, Russian Federation.*

Fax: +7 (496) 514 3244. E-mail: budyka@icp.ac.ru

^b*Branch of the Institute of Energy Problems for Chemical Physics, Russian Academy of Sciences,
142432 Chernogolovka, Moscow Region, Russian Federation*

Photochemical activity of azidohemicyanine (1-methyl-4-(4-azidostyryl)quinolinium iodide) was predicted by quantum chemical calculations and confirmed experimentally. The azidohemicyanine, which was synthesized, is characterized by a long-wavelength absorption band (LWAB) in the spectral region 350–500 nm with a maximum at 417 nm; it decomposes with a quantum yield of 0.84 ± 0.17 upon irradiation within the LWAB, the quantum yield being independent of the presence of oxygen. The reaction products identified by ESI mass spectrometry include the corresponding primary amine as well as azo, hydrazo, nitroso, and nitro compounds, some of them are unidentified. The azidohemicyanine possesses the longest-wavelength visible light sensitivity among aromatic azides known so far.

Key words: quantum chemical calculations, PM3 method, density functional theory, hemicyanine, aromatic azide, photodissociation, quantum yield, light sensitivity, ESI mass spectrometry.

Aromatic azides are widely used as photoaffinity labels^{1–3} and agents for photodynamic therapy.⁴ Most azides used at present are sensitive to hard UV radiation (250–320 nm). At the same time, in the photoaffinity modifications of biomacromolecules it is desirable to expose the system under study to soft long-wavelength UV radiation (350–400 nm) or to visible light (which is better) in order to prevent its photodegradation. To this end, the azide should have an absorption band in the specified spectral region and decompose with high quantum yield upon irradiation with light in this spectral region.

There are a few azido dyes (phenanthridine and acridine derivatives) sensitive to short-wavelength visible light. For instance, azidoethidium dyes decompose with quantum yields from 0.5 to 1.0 on exposure to light with $\lambda = 436$ nm.⁵ 9-Azidoacridinium has a long-wavelength absorption band (LWAB) in the region 400–470 nm and decomposes with a quantum yield of 0.7–1.0 upon irradiation within the LWAB region.⁶ However, this compound is readily hydrolyzed with the formation of acridone in the presence of trace amounts of water, which makes practical application of 9-azidoacridinium difficult. 9-(4-Azidophenyl)acridinium has an absorption band in the same spectral region and is more stable to hydrolysis, but the quantum yield of its photodissociation is very low (<0.01).^{7,8} Other azido dyes that have absorption bands in the longer-wavelength region are also insensitive to light.⁹ It should be noted that all azido

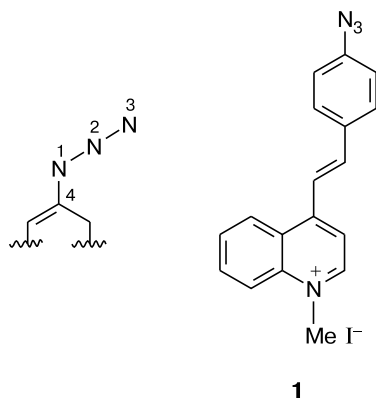
dyes studied so far have a positively charged aromatic nucleus, *i.e.*, they are cations.

Quantum chemical calculations of aromatic azides with different structures and photochemical properties showed^{10,11} that the azide photoactivity is governed by the type of the molecular orbital (MO) that is filled in the lowest singlet-excited state S_1 . If the σ_{NN}^* -MO (antibonding orbital with respect to the N–N(2) bond) is filled, the azide is photoactive (quantum yield, ϕ , of its photodissociation is higher than 0.1). In turn, filling of the σ_{NN}^* -MO depends on the size and charge of the aromatic π -system. If the π -system extends beyond a certain threshold, the σ_{NN}^* -MO in the S_1 state remains vacant and the azide becomes photoinert (ϕ values decrease to less than 0.01). Filling of different-type orbitals leads to different structures of the azide group in the S_1 state of photoactive and photoinert azides, whereas in the ground state (S_0) both types of azides have structurally similar azide groups. Calculations¹² of a series of cata-condensed heteroaromatic azides revealed that the threshold number of π -electrons (photoactivity loss threshold) equals 22 for neutral and 18 for positively charged azides, respectively. As this number is exceeded, the azide photoactivity ceases.

The number of π -electrons in azido derivatives of cyanine and triphenylmethane dyes studied earlier^{9,11} is larger than these threshold values; as a consequence, all these compounds appeared to be photoinert. At the same time it is the hemicyanine π -system that includes 18 elec-

trons; therefore, it was of interest to apply the photoactivity criterion to azidohemicyanine using a theoretical approach developed earlier.

To this end, in the present study we have carried out semiempirical (PM3) and density functional (B3LYP/6-31G*) quantum chemical calculations of 4-(4-azidostyryl)-1-methylquinolinium iodide (azidohemicyanine **1**) in the ground (S_0) and lowest-lying singlet excited (S_1) states. The structural formula of **1** and the atomic numbering scheme are given below. The S_1 state of the azidohemicyanine molecule is characterized by filling of the σ_{NN^*} -MO, which suggests that this compound is photochemically active (see a preliminary communication¹³).



This conclusion was confirmed experimentally. Compound **1** was synthesized; it is characterized by a LWAB in the region 350–500 nm with a maximum at 417 nm. The quantum yield of photodissociation of **1** is 0.84 ± 0.17 irrespective of the presence of oxygen and the irradiation wavelength (365, 379, or 385 nm). The photolysis products identified by ESI mass spectrometry include a conventional mixture typical of photochemistry of arylazides, namely, the corresponding primary amine as well as azo, hydrazo, nitroso, and nitro compounds.

Experimental

Quantum chemical calculations were carried out by the semiempirical method PM3¹⁴ (MOPAC-2002 program package) and using the density functional theory (B3LYP functional, 6-31G* basis set, GAUSSIAN-03 program package¹⁵). The azide geometries in the S_0 and S_1 states were calculated with full geometry optimization. Excited-state calculations were carried out by the PM3 method with inclusion of configuration interaction (CI = 7, eight electrons in seven orbitals, 1225 configurations).

Electronic absorption spectra were measured on a Specord M-40 spectrophotometer and IR spectra were recorded on a Spectrum BX-2 FT-IR spectrometer (KBr pellets). ¹H NMR spectra were recorded on a Bruker DPX-200 spectrometer in DMSO-*d*₆ with Me₄Si as the internal standard.

ESI mass spectra were obtained using an original time-of-flight mass spectrometer with orthogonal ion inlet¹⁶ (positive ion detection).

Solvents were purified using conventional procedures.¹⁷ Ethanol ("distilled, highest purity" grade) was distilled prior to use.

Synthesis of (*E*)-4-(4-azidostyryl)-1-methylquinolinium iodide (1**)** (the reaction and purification were carried out under red light). To a solution of (*E*)-4-(4-azidostyryl)quinoline¹⁸ (60 mg) in anhydrous MeCN (5 mL), MeI (0.5 mL) was added and the reaction mixture was heated at 40 °C for 5 h and then kept at 20 °C for 12 h. To the cooled reaction mixture, petroleum ether (5 mL) was added and the precipitate was filtered off and recrystallized from MeCN–petroleum ether. The yield was 80%, brown-yellow crystals, decomp. temp. 185 °C. ESI MS, found: m/z 287.110 [M]⁺. C₁₈H₁₅N₄⁺. Calculated: M = 287.130. IR, ν/cm^{-1} : 2127 (N₃); 1593, 1567 (CH=CH); 1424, 1369 (CH₃), 837 (*p*-C₆H₄). ¹H NMR, δ : 9.4, 9.15 (both d, 1 H, quinoline H, J = 9 Hz); 7.9–8.7 (m, 8 H, quinoline H, C₆H₄, CH=CH); 7.25 (d, 2 H, C₆H₄, J = 8 Hz); 4.62 (s, 3 H, Me).

A DRS-500 mercury lamp was used as the source of UV light. The 365-nm spectral line was cut using UFS-6 and BS-7 filters. An SDK-470 ultrabright light-emitting diode (emission band with a maximum at λ = 463 nm and a half-width of 20 nm) was used as the source of visible light. A band with a maximum at λ = 479 nm was cut using a ZhS-16 light filter. From the light generated by a KGM-24-250 halogen lamp, a band with a maximum at λ = 485 nm and a half-width of 8 nm was cut using a ZhS-12 glass filter and an IF-475 interference filter.

Photochemical studies were carried out at room temperature in air-saturated or degassed solutions (in the latter case, three freezing–evacuation (down to 0.01 Torr)—thawing cycles were used). The azide concentration in the solutions was $(2\text{--}20) \cdot 10^{-5}$ mol L^{−1}, the optical path length in quartz cells was l = 1 cm, and the light intensity was $(5\text{--}50) \cdot 10^{-10}$ Einstein cm^{−2} s^{−1} (measured using a PP-1 cavity or a ferrioxalate actinometer).

Results and Discussion

Molecular and electronic structure of the azidohemicyanine. Selected geometric parameters and electronic characteristics of the S_0 and S_1 states of the azidohemicyanine optimized by the B3LYP/6-31G* and PM3 methods are listed in Table 1. Similarly to azides studied earlier,^{10–12} the azido group in molecule **1** has a quasi-linear geometry (N–N–N bond angle is nearly 170°) and the terminal nitrogen atoms bear large positive charges. Compared to B3LYP/6-31G*, the PM3 method somewhat overestimates the atomic charges and bond lengths.

Excited-state calculations revealed a bending geometry of the azido group and elongation of the N(1)–N(2) bond by 0.122 Å accompanied by a decrease in the order of this bond by a value of 0.39; in addition, the charge on the terminal N₂ group decreases (see Table 1). As mentioned earlier,¹¹ this pattern of changes in the parameters on going from the S_0 to S_1 state are characteristic of photoactive azides.

Changes in the geometric parameters upon excitation depend on the type of the orbitals participating in the electron transfer process. The compositions of the (i) frontier MOs, namely, the highest occupied MO (HOMO) and the lowest unoccupied MO (LUMO) in

Table 1. N(1)—N(2) and C(4)—N(1) bond lengths (r), bond orders (overlap populations) (p), N(1)—N(2)—N(3) bond angles (ω_{NNN}), and the Mulliken effective charges on the terminal N₂ group (Z_{N_2}) in the ground state (S_0) and in the lowest-lying electron-excited (S_1) state of azidohemicyanine **1** calculated using different methods (with no counterion)

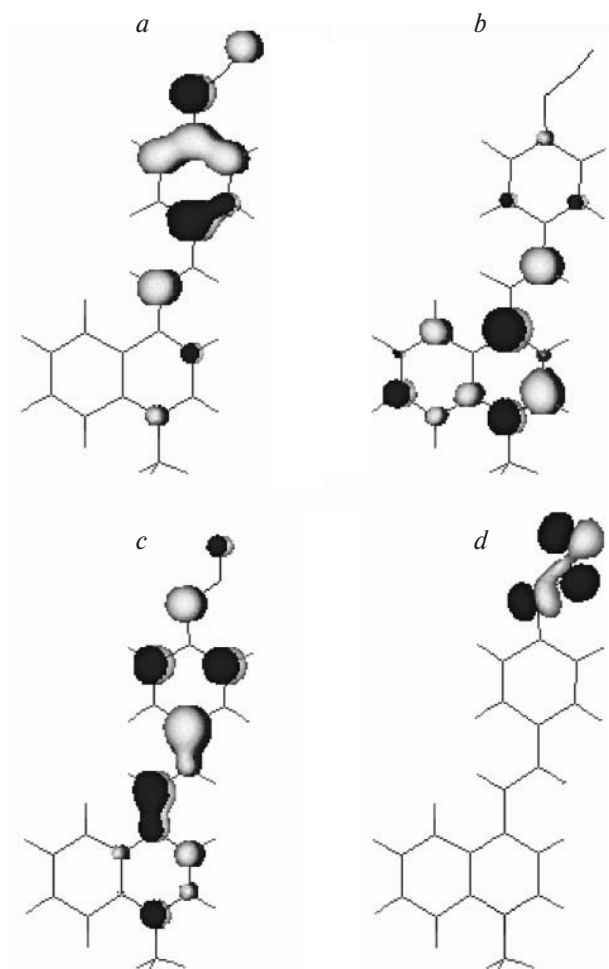
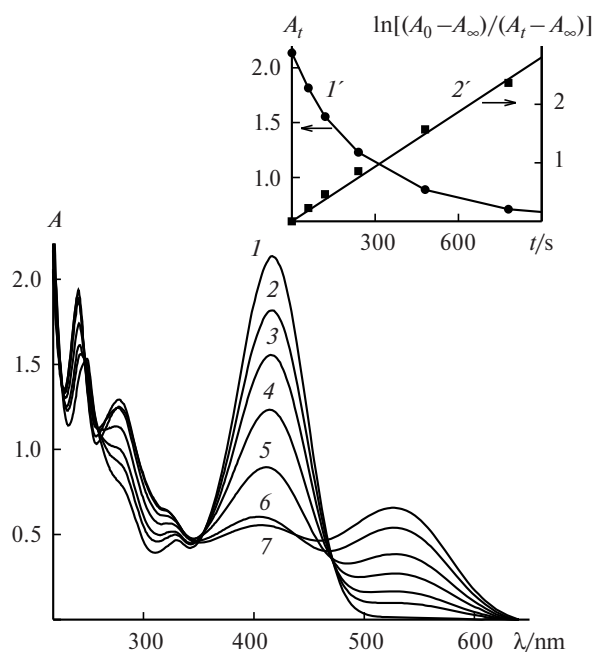
State	Computational method	$r/\text{\AA}$		p		$\omega_{\text{NNN}}/\text{deg}$	Z_{N_2}/e
		N(1)—N(2)	C(4)—N(1)	N(1)—N(2)	C(4)—N(1)		
S_0	PM3	1.278	1.419	1.29	1.06	169.5	0.45
S_0	B3LYP/6-31G*	1.247	1.399	0.48	0.57	171.8	0.26
S_1	PM3	1.400	1.316	0.90	1.66	129.5	0.17

the S_0 state and (ii) the lowest and highest singly occupied MOs (LSOMO and HSOMO, respectively) in the S_1 state are shown in Fig. 1. In the S_0 state both frontier MOs are π -orbitals localized on the aromatic nuclei and on the central double bond. The σ_{NN}^* -MO of interest is localized on the azido group, being antibonding in character with respect to the N—N(2) bond. Its energy level lies 3.26 eV higher than that of the LUMO and the σ_{NN}^* -MO

itself is the LUMO+7 orbital (according to PM3 calculations).

However, it is the σ_{NN}^* -MO rather than the aromatic π -MO (formerly LUMO) that is filled in the relaxed S_1 state (see Fig. 1), which is a prerequisite for photodissociation of the azido group. This suggests that the azidohemicyanine will decompose on exposure to light within the LWAB with a quantum yield $\phi > 0.1$, *i.e.*, be a photo-active azide.

The kinetics of photolysis. The spectral changes upon irradiation of a degassed solution of azide **1** in EtOH at 485 nm are shown in Fig. 2 as an example. The absorption spectrum of the initial compound (spectrum 1) exhibits an intense band with a maximum at $\lambda = 417$ nm (molar extinction coefficient $\epsilon = 28900 \text{ L mol}^{-1} \text{ cm}^{-1}$)

**Fig. 1.** Frontier MO compositions for azidohemicyanine **1**: HOMO (a) and LUMO (b) in the S_0 state; LSOMO (c) and HSOMO (d) in the S_1 state.**Fig. 2.** Spectral changes in the course of photolysis of degassed solution of azidohemicyanine **1** in EtOH ($7.4 \cdot 10^{-5} \text{ mol L}^{-1}$) at $\lambda = 485 \text{ nm}$; light intensity $I_0 = 1.08 \cdot 10^{-9} \text{ einstein cm}^{-2} \text{ s}^{-1}$, photolysis duration: 0 (1), 60 (2), 120 (3), 240 (4), 480 (5), 1380 (6), and 2900 s (7). The inset shows the kinetics of changes in the optical density at 417 nm (I') and its semilogarithmic anamorphose ($2'$).

and a long-wavelength tail spanning to 500 nm in the visible region, and two weaker bands at 332 (ϵ 6100 L mol⁻¹ cm⁻¹) and 249 nm (ϵ 19600 L mol⁻¹ cm⁻¹) in the UV region (see Fig. 2, spectrum 1). Upon irradiation, the short-wavelength band is shifted to 240 nm, the long-wavelength band disappears, and two new bands appear near 280 and 530 nm (spectra 2–7).

The isosbestic points at 246.9, 354.1, and 471.7 nm (see Fig. 2) retained their positions in the initial stage of photolysis and gradually shifted on further irradiation. Some kinetic curves showed extrema, *e.g.*, the optical density near 280 nm initially increased, passed through a maximum, and then decreased. In addition, the optical density of the reaction product near 530 nm continued to increase after the intensity of the azide band at 417 nm no longer decreased. These data suggest that the products of azide photolysis undergo subsequent reactions.

The occurrence of several reactions in the system clearly manifested itself in analysis of the spectral changes by the method of principal components (spectral data processing program is described in Ref. 19). The score plot representing the experimental spectra shown in Fig. 2 in the basis set of the first three singular vectors is presented in Fig. 3. Each point in Fig. 3 corresponds to a particular spectrum of the reaction mixture shown in Fig. 2; the analysis was performed for the spectral region from 40000 to 16480 cm⁻¹ with an increment of 80 cm⁻¹, *i.e.*, the initial matrix included 295 optical density values for each of the seven spectra. The initial linear region of the plot (see Fig. 3, solid line) means that only one reaction resulting in a single compound or several concurrent reactions at constant relative proportion of products-components (only their concentrations vary) occur in this stage of azide photolysis. Deviation of the next point-spectrum from the initial linear region implies vio-

lation of the ratio of the component concentrations at this instant. This corresponds to the "switching on" a new reaction or "switching off" a certain concurrent reaction.

Considering the azidohemicyanine structure, it is logical to assume that here we deal with the second case where consumption of the azide is followed by "switching off" the photodissociation of the azido group, but photoisomerization of the central double bond of the styryl fragment in the azide photolysis products still does occur. Since cyanine dyes are prone to formation of various complexes and aggregates,²⁰ this process can also contribute to the mismatch of the kinetic curves measured at different wavelengths.

For comparison, in Fig. 3 we present the results of analysis of the reaction mixture using the method of principal components taking photolysis of an air-saturated solution of azide 1 (dotted curve) as an example. In this case, we also observed the initial linear region followed by gradual deviation of points from the straight line on further irradiation, *i.e.*, secondary reactions occurred. The mismatch of the initial points in the curves (see Fig. 3) can be explained by small changes in the azide absorption spectrum on degassing and the mismatch of the curves on the whole points to formation of different products in the presence and in the absence of oxygen (see below).

To simplify the procedure for processing of the kinetic curves, photolysis of azide 1 was carried out following two different light-absorption patterns. When the sample was photolyzed at 365 nm, conditions for almost 100% light absorption (optical density at the irradiation wavelength $A_{\text{ex}} > 1$) were met in the very beginning of the process. In this case, the quantum yield of azide decomposition was calculated from the slope of the initial linear region of the kinetic curve using the equation

$$A_t = A_0 - \epsilon_\lambda \phi I_0 t (A_0 - A_\infty) / A_0, \quad (1)$$

where A_t , A_0 , and A_∞ are the optical densities of the reaction mixture at the observation wavelength λ at the instant t , at $t = 0$, and after completion of the process (A_∞ value was estimated at long photolysis times); ϵ_λ is the extinction coefficient of azidostyrylquinoline (L mol⁻¹ cm⁻¹) at the observation wavelength; and I_0 is the intensity of incident light (Einstein cm⁻² s⁻¹). The maximum of the azide LWAB was used as the observation wavelength.

Photolysis with visible light at the edge of the long-wavelength tail of the absorption band corresponded to a reaction in a thin optical layer (optical density at the irradiation wavelength $A_{\text{ex}} < 0.1$). The quantum yield ϕ was calculated from the equation

$$\ln[(A_0 - A_\infty)/(A_t - A_\infty)] = 2.3 \epsilon_{\text{ex}} \phi I_0 t, \quad (2)$$

where ϵ_{ex} is the extinction coefficient of azidostyrylquinoline (L mol⁻¹ cm⁻¹) at the irradiation wavelength.

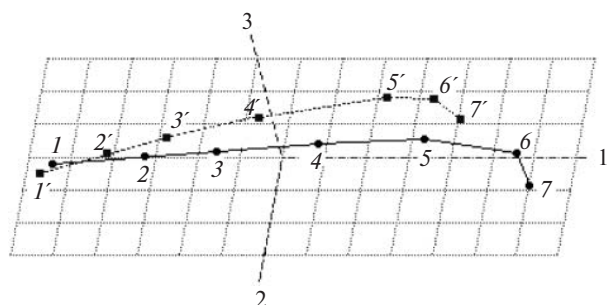


Fig. 3. Analysis of reaction mixture (see Fig. 2) by the method of principal components (solid curve); experimental spectra are presented in the basis set of the first three singular vectors; points 1–7 correspond to the spectra 1–7 in Fig. 2. Analysis of the reaction mixture in the case of photolysis of air-saturated solution of azidohemicyanine 1 by the method of principal components using the same coordinates; points 1'–7' correspond to the spectra recorded at a photolysis duration of 0, 60, 120, 240, 540, 840, and 1500 s, respectively (see text).

The inset (see Fig. 2, curve 2') shows an example of processing of experimental data in the coordinates of Eq. (2).

The quantum yields (ϕ) of photodissociation of azido-hemicyanine **1** in EtOH on exposure to light with different wavelengths and under different photolysis conditions calculated from the kinetic curves are listed below (error is $\pm 20\%$). As can be seen, azide **1** exposed to light with the wavelength within the LWAB decomposes with a high quantum yield irrespective of the presence of oxygen and irradiation wavelength; the average ϕ value is 0.84 ± 0.17 .

$\lambda_{\text{ex}}/\text{nm}$	365	365	479	485	485
ϕ	0.80	0.86*	0.89	0.85	0.80*

* Degassed solution.

Reaction products. Usually, photolysis of aryl azides results in the corresponding primary and secondary amines, as well as azo, hydrazo, azoxy, nitroso, and nitro compounds, *etc.*²¹ The percentage of these compounds in the reaction mixture depends on the initial azide concentration²² and therefore the results of preparative photolysis of concentrated solutions cannot directly be applied to dilute solutions used in spectral studies.

Using ESI mass spectrometry, we have analyzed dilute reaction mixtures (concentrations $\sim 10^{-5}$ mol L⁻¹) used in the kinetic studies when measuring the quantum yields, determined the compositions of the reaction mixtures at different durations of irradiation of the solutions of azide **1**, and compared them with spectrophotometric data. The results obtained are presented in Table 2.

In the initial stage of photolysis corresponding to the absorption spectrum **3** in Fig. 2 (azide conversion

20–25%), the reaction mixture contained two major components, the initial azide characterized by the most abundant peak in the mass spectrum (m/z 287, 100%) and the corresponding primary amine (m/z 261, 59%); peaks of other compounds were more than tenfold weaker (see Table 2). Therefore, in this stage the amine can be considered as the only reaction product; this is consistent with the isosbestic points in the absorption spectra at a given instant (see Fig. 2, spectra **1**–**4**). This amine, (*E*)-4-(4-aminostyryl)-1-methylquinolinium iodide, is the simplest hemicyanine dye characterized by a LWAB near 530 nm in the absorption spectra of photolysis products.

In addition to the amine, the degassed solution contained the following final reaction products: the corresponding azo compound (m/z 259 [M]²⁺, doubly charged ion, $M = 518$) and a hydrazo compound (m/z 260 [M]²⁺, doubly charged ion, $M = 520$). The mass spectrum also exhibits weaker peaks of unidentified products with m/z 218.097, 229.593 ([M]²⁺, doubly charged ion, $M = 459$) and 295.080 (see Table 2), which can be attributed to secondary reaction products.

When photolysis was carried out in the presence of oxygen, the amine remained the major reaction product, the percentages of the amine, azo, and hydrazo compounds being almost unchanged (100, 62, and 8%, respectively). In addition, oxygen-containing products formed including the corresponding nitroso (m/z 275), nitro (m/z 291), and azoxy compounds (m/z 267, [M]²⁺, doubly charged ion, $M = 534$), as well as the same unidentified products as in the degassed solution (see Table 2).

It is noteworthy that the percentages of the nitroso and nitro compounds in the photolysis of azido-hemicyanine

Table 2. Relative peak intensities (I/I_{max} (%)) in ESI mass spectra of the photolysis products of azido-hemicyanine solutions irradiated at $\lambda = 365$ nm

Product ^a	Structure ^a	m/z	I/I_{max} (%)	
			Air-saturated solution	Degassed ^b solution
C ₁₈ H ₁₇ N ₂ ⁺	QuSt–NH ₂	261.116	100	100 (59)
C ₁₈ H ₁₅ N ₂ O ⁺	QuSt–NO	275.098	9	—
C ₁₈ H ₁₇ N ₂ O ⁺	QuSt–NHOH	277.090	6	5 (—)
C ₁₈ H ₁₇ N ₂ O ₂ ⁺	QuSt–NO ₂	291.099	4	—
C ₃₆ H ₃₀ N ₄ ²⁺	QuSt–N=N–StQu	259.099	63	62 (60)
C ₃₆ H ₃₂ N ₄ ²⁺	QuSt–NH–NH–StQu	260.106	8 ^c	8 ^c (—)
C ₃₆ H ₃₀ N ₄ O ²⁺	QuSt–N=N(O)–StQu	267.097	6	—
— ^d	—	218.097	17	15 (2)
— ^d	—	229.593	5	14 (—)
— ^d	—	295.080	14	15 (5)

^a Shown are the molecular formulas with no anions; for the structures, see Scheme 1.

^b The results of analysis of the reaction mixture in the initial stage of photolysis (azide peak with m/z 287.105 is the strongest in the mass spectrum) are given in parentheses.

^c Peak intensity corrected for the isotope peak [M + 2] of the azo compound ion.

^d Unidentified product.

1 (9 and 4%, respectively) are almost an order of magnitude lower than in the photolysis of neutral (*E*)-4-(4-azidostyryl)quinoline, a precursor of azide **1** (60 and 40%, respectively²³). This can be due to the decrease in the nitrene reactivity towards oxygen as a result of partial localization of positive charge on the nitrene nitrogen atom. At the same time, the positive charge does not prevent nitrene dimerization to the azo compound because the doubly charged ion peak of this product with m/z 259 in the mass spectra in all cases is the next in intensity (see Table 2).

The mass spectrum of the solution also exhibits a peak with m/z 259 (see Table 2) in the initial stage of photolysis; however, here this is the peak of nitrene (product of azide decomposition in the ionizing field). The m/z value of the nitrene peak is the same as that of the azo compound peak (259), but the former originates from the singly while the latter originates from the doubly charged ion; therefore, one can distinguish between these peaks with ease using the parameters of isotope peaks, namely, the m/z value and peak intensity. The nitrene isotope peak $[M + 1]$ has m/z 260.127 and a relative intensity of 19.5%, whereas the azo compound isotope peak has m/z 259.625 and a doubled intensity (38.8%).

The regions in the mass spectra for the mass range under study for the two reaction mixtures in the initial and final stages of photolysis are shown in Fig. 4. The lack of peaks with half-integer mass in the former case (see Fig. 4, *a*) and the presence of these peaks in the latter case (see Fig. 4, *b*), as well as their relative intensities allow the peak with m/z 259 to be unambiguously assigned to nitrene in the former and to the azo compound in the latter case.

The ion peak with m/z 277 in the mass spectra corresponds to both the hydroxyamino derivative and substi-

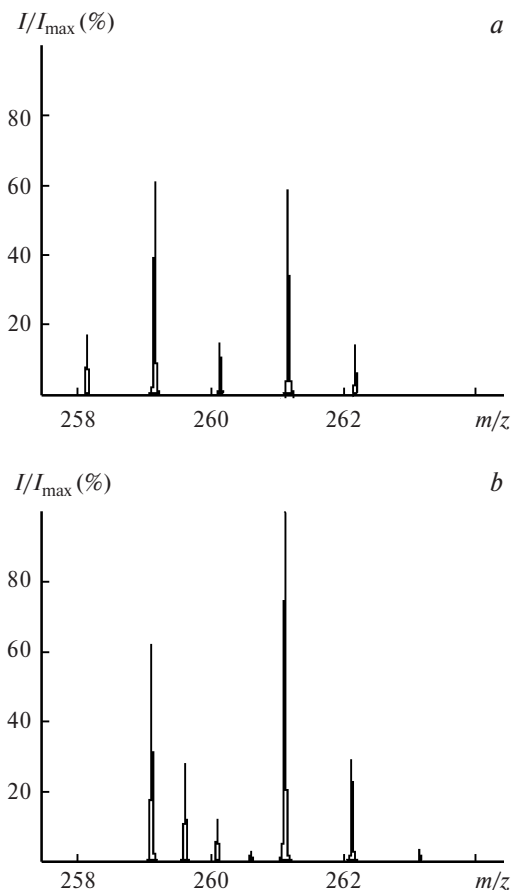
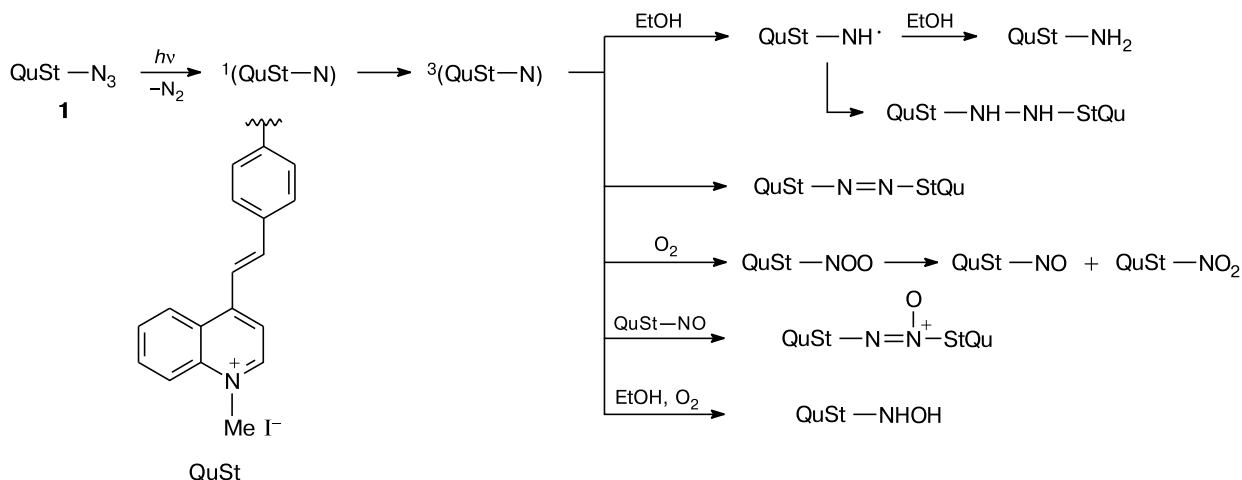


Fig. 4. Mass spectra of reaction mixtures in photolysis of azidohemicyanine **1** in EtOH: *a* — initial stage of photolysis, the peak with m/z 259 corresponds to nitrene (azide peak with m/z 287 is the strongest in the mass spectrum); *b* — final stage of photolysis, the peak with m/z 259 corresponds to the azo compound (no azide peak in the spectrum). The peaks with m/z 261 in both spectra correspond to amine.

Scheme 1



tuted aminophenol. It is noteworthy that the formation of this compound is almost independent of the presence of oxygen (see Table 2), namely, different compounds with the same m/z value can probably form under different conditions.

On the whole, the formation of all identified products in the photolysis of azidohemicyanine **1** can be explained by the reactions of the triplet nitrene²¹ (Scheme 1).

Thus, our studies confirmed the predicted photochemical activity of azides with positively charged conjugated π -system including at most eighteen electrons. Azidohemicyanine (4-(4-azidostyryl)-1-methylquinolinium iodide) was synthesized for the first time. The compound has a LWAB in the region 350–500 nm and decomposes with a quantum yield of 0.84 ± 0.17 irrespective of the presence of oxygen on exposure to light within the LWAB. Among the known aromatic azides, the azidohemicyanine possesses the longest-wavelength visible light sensitivity and is characterized by the high quantum yield of photodissociation of the azido group.

The authors are grateful to A. G. Ryabenko for providing the program for analysis of spectral data by the method of principal components.

This work was financially supported by the Russian Foundation for Basic Research (Project No. 03-03-32116).

References

1. U. Henriksen, O. Buchardt, P. E. Nielsen, *J. Photochem. Photobiol. A: Chem.*, 1991, **57**, 331.
2. R. S. Pandurangi, R. R. Kuntz, W. A. Volkert, *Appl. Radiat. Isotopes*, 1995, **46**, 233.
3. M. J. Bouchet, M. Goeldner, *Photochem. Photobiol.*, 1997, **65**, 195.
4. R. Rajagopalan, G. Cantrell, S. I. Achilefu, J. E. Bugai, R. B. Dorshow, US Pat. 2004/0180864.
5. N. P. Gritsan, A. A. Koshkin, A. Yu. Denisov, Yu. Ya. Markushin, E. V. Cherepanova, A. V. Lebedev, *J. Photochem. Photobiol. B: Biol.*, 1997, **37**, 40.
6. M. F. Budyka, N. V. Biktimirova, T. N. Gavrishova, *Khim. Vys. Energ.*, 2006, **40**, 208 [*High Energy Chem.*, 2006, **40**, 170 (Engl. Transl.)].
7. M. F. Budyka, M. M. Kantor, R. M. Fatkulbayanov, *Khim. Geterotsikl. Soedin.*, 1997, 1504 [*Chem. Heterocycl. Compd.*, 1997, **33** (Engl. Transl.)].
8. M. F. Budyka, N. V. Biktimirova, T. N. Gavrishova, O. D. Laukhina, *Izv. Akad. Nauk. Ser. Khim.*, 2005, 2655 [*Russ. Chem. Bull., Int. Ed.*, 2005, **54**, 2746].
9. V. Ya. Pochinok, V. A. Smirnov, S. B. Brichkin, L. F. Avramenko, L. I. Tytlina, T. F. Grigorenko, I. A. Ol'shevskaya, V. N. Skopenko, *Ukr. Khim. Zh.* [*Ukr. Chem. J.*], 1984, **50**, 296 (in Russian).
10. M. F. Budyka, T. S. Zyubina, *J. Mol. Struct. (Theochem.)*, 1997, **419**, 191.
11. M. F. Budyka, T. S. Zyubina, M. M. Kantor, *Zh. Fiz. Khim.*, 2000, **74**, 1115 [*Russ. J. Phys. Chem.*, 2000, **74**, 995 (Engl. Transl.)].
12. M. F. Budyka, I. V. Oshkin, *J. Mol. Struct. (Theochem.)*, 2006, **759**, 137.
13. M. F. Budyka, N. V. Biktimirova, T. N. Gavrishova, V. I. Kozlovskii, *Mendeleev Commun.*, 2007, **17**, 3.
14. J. J. P. Stewart, *J. Comput. Chem.*, 1989, **10**, 208, 221.
15. M. J. Frisch, G. W. Trucks, H. B. Schlegel, G. E. Scuseria, M. A. Robb, J. R. Cheeseman, J. A. Montgomery, Jr., T. Vreven, K. N. Kudin, J. C. Burant, J. M. Millam, S. S. Iyengar, J. Tomasi, V. Barone, B. Mennucci, M. Cossi, G. Scalmani, N. Rega, G. A. Petersson, H. Nakatsuji, M. Hada, M. Ehara, K. Toyota, R. Fukuda, J. Hasegawa, M. Ishida, T. Nakajima, Y. Honda, O. Kitao, H. Nakai, M. Klene, X. Li, J. E. Knox, H. P. Hratchian, J. B. Cross, C. Adamo, J. Jaramillo, R. Gomperts, R. E. Stratmann, O. Yazyev, A. J. Austin, R. Cammi, C. Pomelli, J. W. Ochterski, P. Y. Ayala, K. Morokuma, G. A. Voth, P. Salvador, J. J. Dannenberg, V. G. Zakrzewski, S. Dapprich, A. D. Daniels, M. C. Strain, O. Farkas, D. K. Malick, A. D. Rabuck, K. Raghavachari, J. B. Foresman, J. V. Ortiz, Q. Cui, A. G. Baboul, S. Clifford, J. Cioslowski, B. B. Stefanov, G. Liu, A. Liashenko, P. Piskorz, I. Komaromi, R. L. Martin, D. J. Fox, T. Keith, M. A. Al-Laham, C. Y. Peng, A. Nanayakkara, M. Challacombe, P. M. W. Gill, B. Johnson, W. Chen, M. W. Wong, C. Gonzalez, J. A. Pople, *Gaussian 03, Revision B.02*, Gaussian Inc., Pittsburgh, PA, 2003.
16. A. F. Dodonov, V. I. Kozlovskii, I. V. Soulimenkov, V. V. Raznikov, A. V. Loboda, Z. Zhen, T. Horwath, H. Wollnik, *Eur. J. Mass Spectrom.*, 2000, **6**, 481.
17. *Svoistva organicheskikh soedinenii. Spravochnik*, pod red. A. A. Potekhina, Khimiya, Moscow, 1984, 520 pp. (in Russian).
18. M. F. Budyka, N. V. Biktimirova, T. N. Gavrishova, *Khim. Vys. Energ.*, 2007, **41**, 115 [*High Energy Chem.*, 2007, **41**, 84 (Engl. Transl.)].
19. A. G. Ryabenko, E. E. Faingol'd, E. N. Ushakov, N. M. Bravaya, *Izv. Akad. Nauk. Ser. Khim.*, 2005, 2257 [*Russ. Chem. Bull., Int. Ed.*, 2005, **54**, 2330].
20. L. K. Gallos, E. Stathatos, P. Lianos, P. Argyrakis, *Chem. Phys.*, 2002, **275**, 253.
21. *Azides and Nitrenes. Reactivity and Utility*, Ed. E. F. V. Scriven, Academic Press, New York, 1984.
22. M. F. Budyka, M. M. Kantor, M. V. Alfimov, *Usp. Khim.*, 1992, **61**, 48 [*Russ. Chem. Rev.*, 1992, **61** (Engl. Transl.)].
23. M. F. Budyka, N. V. Biktimirova, T. N. Gavrishova, V. I. Kozlovskii, *Khim. Vys. Energ.*, 2007, **41**, 305 [*High Energy Chem.*, 2007, **41**, 261 (Engl. Transl.)].

Received May 31, 2007;
in revised form June 4, 2007